

Polarimetric mapping of a new infrared reflection nebula GGD 27 IRS

T. Yamashita¹, S. Sato^{2*}, T. Nagata^{1**}, H. Suzuki³, J.H. Hough⁴, I.S. McLean^{5***}, R. Garden⁶, and I. Gatley^{7****}

¹ Department of Physics, Kyoto University, Sakyou-ku Kyoto 606, Japan

² Institute for Astronomy, University of Hawaii, 2680 Woodlawn Drive, Honolulu, HI 96822, USA

³ Nobeyama Radio Observatory, Tokyo Astronomical Observatory, Minamisaku, Nagano 384–13, Japan

⁴ Physics Department, Hatfield Polytechnic, Hatfield, Hertfordshire AL109AB, UK

⁵ Royal Observatory, Blackford Hill, Edinburgh EH9 3HJ, Scotland

⁶ University of Edinburgh, Blackford Hill, Edinburgh EH9 3HJ, Scotland

⁷ United Kingdom Infrared Telescope Unit, 665 Komohana St., Hilo, HI 96720, USA

Received October 24, accepted November 28, 1986

Summary. We report the discovery of an infrared reflection nebula GGD 27 IRS, near the optical nebulosity GGD 27. It shows a dumbbell-shaped structure with large degrees of polarization, up to 64%, in the *K* band. From the centrosymmetric pattern of the polarization vectors we identify the illuminating source of the nebula with IRS 2. A simple model based on single Rayleigh scattering at the surface of a paraboloidal shell gives good agreement with the observed radial dependence of both polarization and surface brightness. This model is in good agreement with the recently revealed shell structure of the CO bipolar flow. Small polarization and low surface brightness both east and west of IRS 2 indicate the presence of a disk of obscuring material elongated orthogonal to the extent of the nebula. We estimate the size, extinction, and mass of the disk to be $40'' \times 60''$, 75 mag and $200 M_{\odot}$, respectively.

Key words: star formation – reflection nebulae – infrared radiation – polarization

1. Introduction

Recent polarization maps (Tokunaga et al., 1981; Werner et al., 1983; Heckert and Zeilik, 1984; Lenzen et al., 1984; Joyce and Simon, 1986) have established the presence of infrared reflection nebulae associated with young stellar objects (YSOs). They show large polarization, typically 50%, and elongated or bipolar structure in their surface brightness. Although a scattering model is accepted as a polarization mechanism, the detailed geometry of the scattering field has not been understood yet. For the central source of CO bipolar flows Hodapp (1984) and Sato et al. (1985)

constructed a model with the scattering material located above an obscuring disk on the basis of the orthogonality between the infrared polarization and CO bipolar flows.

Heckert and Zeilik (1985) made a model calculation by using a simple geometry, that is, an optically thin bipolar lobe surrounding an optically thick torus, in order to explain the wavelength dependence of infrared polarization. However, the polarization measured on the intensity peak is rather insensitive to the exact geometry. Although spatially resolved polarization maps would provide a diagnostic for the geometry of the radiation field, previous observations do not provide any good examples suitable for detailed examination in a sense that most of them (i) are not viewed nearly edge-on, (ii) include several luminous sources, or (iii) show rather large irregularities in the nebula, presumably due to clumpiness of the scatterers. The present observations show this new infrared source, GGD 27 IRS, to be a particularly good example with the above difficulties relatively insignificant. By examining this source we discuss the geometries around it in the light of the latest discovery of a shell structure of the CO bipolar flow in L1551 dark cloud (Snell et al., 1985; Uchida et al., 1987).

GGD 27 is located at the south-western edge of a dark lane extending in the NW-SE direction in Sagittarius. It was thought to be a Herbig-Haro candidate from its appearance on the Palomar Observatory Sky Survey (Gyulbudaghian et al., 1978). Hartigan and Lada (1985) showed it not to be a Herbig-Haro object but a reflection nebulosity from the lack of $H\alpha$ emission. Rodriguez et al. (1980) found a weak radio continuum at 5 GHz, and an H_2O and an OH maser close to GGD 27. They also detected ^{12}CO , ^{13}CO , and NH_3 molecules and derived a kinematic distance of 1.7 kpc from the velocity of ^{12}CO . The flux of the radio continuum corresponds to an exciting star of B1V at the distance of 1.7 kpc. Yamashita et al. (1987) mapped this region with CO and CS lines and found a CO bipolar flow with blue- and red-shifted lobes extending to the north and south, respectively, and a CS disk elongated in the east and west direction.

2. Observations and results

In the course of a *K* band polarization survey with the Agematsu 1 m infrared telescope, we found a highly polarized source in the

Send offprint requests to: T. Yamashita

* On leave from Department of Physics, Kyoto University

** Present address: Institute for Astronomy, University of Hawaii, 2680 Woodlawn Drive, Honolulu, HI 96822, USA

*** Present address: United Kingdom Infrared Telescope Unit, 665 Komohana St., Hilo, HI 96720, USA

**** Present address: Kitt Peak National Observatory, P.O. Box 26732, Tucson, AZ 85726-6732, USA

Table 1. Positions of sources

Sources	R.A. (1950)	Dec. (1950)	K mag	Identification	Reference
IRS 1	$18^{\text{h}}16^{\text{m}}13^{\text{s}}0 \pm 3''$	$-20^{\circ}49'09'' \pm 3''$	8.1		1
IRS 2	$18^{\text{h}}16^{\text{m}}13^{\text{s}}2 \pm 3''$	$-20^{\circ}48'46'' \pm 3''$	9.4	5 GHz cont.	1, 2
IRS 3	$18^{\text{h}}16^{\text{m}}15^{\text{s}}8 \pm 3''$	$-20^{\circ}49'04'' \pm 3''$	9.9	Starlike image	1, 3
IRS 4	$18^{\text{h}}16^{\text{m}}11^{\text{s}}7 \pm 3''$	$-20^{\circ}48'16'' \pm 3''$	10.1	No. 41; GGD 27	1, 3
IRS 5	$18^{\text{h}}16^{\text{m}}11^{\text{s}}7 \pm 3''$	$-20^{\circ}49'13'' \pm 3''$	10.3		1
IRS 6	$18^{\text{h}}16^{\text{m}}10 \pm 10''$	$-20^{\circ}47'54'' \pm 10''$	7.7	Starlike image	1, 3
5GHz cont.	$18^{\text{h}}16^{\text{m}}13^{\text{s}}0$	$-20^{\circ}48'48''$			2
AFGL2121	$18^{\text{h}}16^{\text{m}}18$	$-20^{\circ}45'1$			4
18162-2048	$18^{\text{h}}16^{\text{m}}12^{\text{s}}8$	$-20^{\circ}48'51''$			5
No. 32	$18^{\text{h}}16^{\text{m}}12^{\text{s}}82$	$-20^{\circ}49'08''6$			3

References: (1) This paper; (2) Rodriguez et al., 1980; (3) Hartigan and Lada, 1985; (4) Walker and Price, 1975; (5) IRAS point source catalogue, 1985

vicinity of GGD 27 (we call GGD 27 IRS). Its intensity and the degree of polarization are 8.6 mag and about 20% in the K band, respectively, with a beam of $15''$ and a chopping throw of $60''$ in the east and west direction. The cross scans in the K band indicate an extent as large as $2'$ in the north-south and $1'$ in the east-west directions, respectively.

We made a K band intensity map of this source using the UH 88 inch telescope at Mauna Kea on 4 and 5 July, 1985, with a beam of $8''$ and a chopping throw of $60''$ in the north-south direction. The infrared source, GGD 27 IRS, was spatially resolved into six discrete sources and a diffuse component. The coordinates of the discrete sources are listed in Table 1, together with the positions of sources relevant to GGD 27 IRS. Near infrared photometry of IRS 1 and IRS 2 is presented in Table 2 and in Fig. 3, together with the IRAS data.

Subsequently we carried out polarization mapping in the K and L' bands with the Kyoto Polarimeter on the UKIRT 3.8 m telescope on 25, 26 July and 19, 20 August, 1985. We used beams of $20''$ in the K band and $12''$ in the L' band. A chopping throw of $220''$ in the east-west direction was employed throughout the observations at the UKIRT. In order to check the contamination from field stars in the reference beam, we measured each grid point twice with a reference at either side of east and west. The methods of polarimetry were identical to those of Sato et al. (1987). Instrumental polarization was measured to be less than 0.2%. Position angles were calibrated by observing GL 2591, whose position angle is 171° in the K band (Lonsdale et al., 1980). The polarization maps in the K and L' bands are shown in Figs. 1 and 2, respectively.

The radial dependences of the degree of polarization and surface brightness were also measured with a beam of $12''$ in the K band along a vertical line to the north from IRS 2 and are shown in Figs. 4 and 5.

Table 2. Photometries of IRS 1 and 2

Bands	Magnitude				
	J	H	K	L'	M
IRS 1	13.1	10.3	8.1	5.9	4.9
IRS 2	13.9	12.1	9.4	5.9	4.7

Typical errors for the degree of polarization are 2% in the K band and 3% in the L' band. The signal-to-noise ratio of the flux at the lowest contours are 50 and 20 in the K and L' bands, respectively.

3. Discussion

GGD27 IRS consists of a diffuse component and six sources unresolved with a beam of $8''$. Of these six discrete sources, IRS 3, 4, and 6 are identified with optical images on the CCD frame by

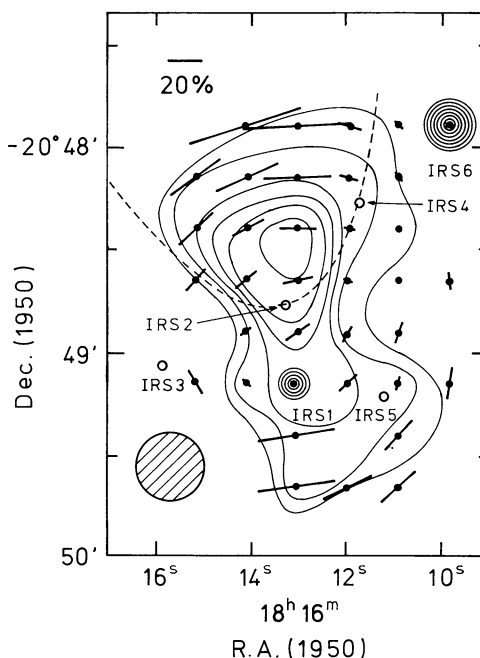


Fig. 1. Surface brightness and polarization map of GGD 27 IRS in the K band. The beam size of $20''$ is indicated by the hatched circle. Contour levels are 1, 2, 3, 5, 7, $10 \cdot 10^{-20} \text{ W cm}^{-2} \mu\text{m}^{-1} \text{ arcsec}^{-2}$, respectively. Each bar indicates the degree and the direction of polarization at the position of its center denoted by a filled circle. A polarization of 20% is displayed by the bar in the upper left corner. Open circles indicate the infrared sources identified with a $8''$ beam. Although IRS 2 is pointlike in the K band with $8''$ resolution, it shows no enhancement in the surface brightness, because extended component is very strong in a $20''$ beam

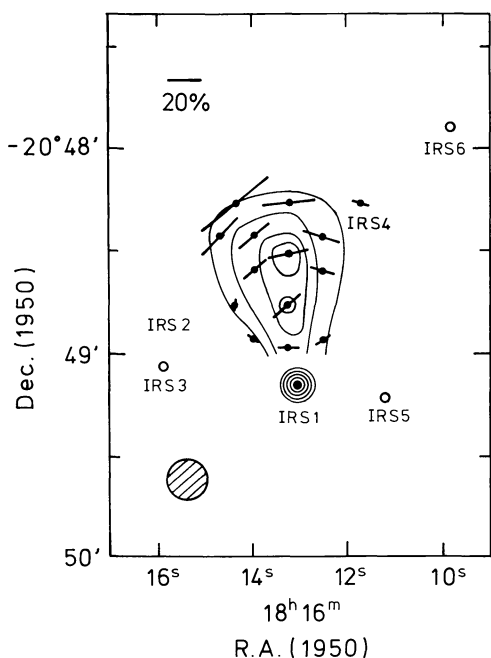


Fig. 2. Surface brightness and polarization map in the L' band of GGD 27 IRS. Designations are the same as in Fig. 1 except the beam size of $12''.4$ and the contour levels of $0.5, 1, 2, 4 \times 10^{-20} \text{ W cm}^{-2} \mu\text{m}^{-1} \text{ arcsec}^{-2}$.

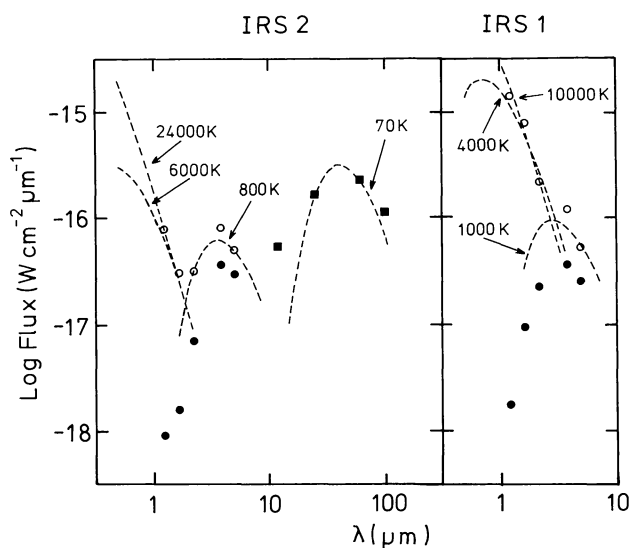


Fig. 3. The energy spectrum of IRS 1 and 2. The filled circles are from our photometry and the filled squares are from IRAS point source catalogue. The open circles are dereddened ones by visual extinctions of 20 mag for IRS 2 and of 30 mag for IRS 1. The dashed lines are blackbody spectra of the temperatures indicated

Hartigan and Lada (1985), as shown in Table 1. IRS 4 coincides with the optical nebulosity GGD 27.

3.1. The diffuse component

The diffuse component shows a dumbbell-shaped structure extending for about $2'$ in the north-south direction. The largest

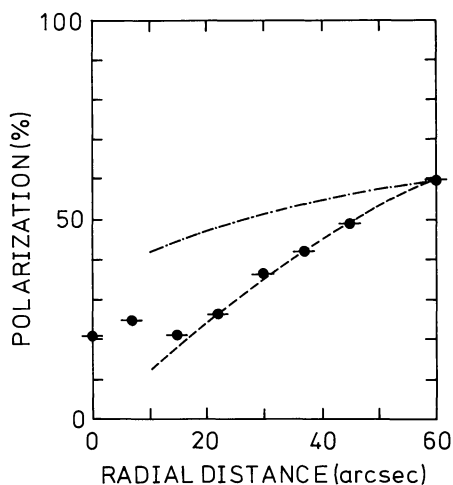


Fig. 4. Radial dependence of the degree of polarization along the vertical line to the north from IRS 2. The positional error is indicated by the horizontal lines. Errors in the degrees of polarization are within the radius of the circles. The dot-dashed and dashed lines show dependences of Rayleigh scattering calculation for volume and surface scattering, respectively. The employed parameters are summarized in Table 3

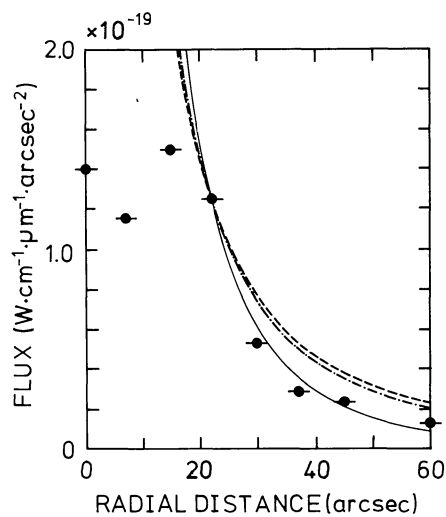


Fig. 5. Radial dependence of surface brightness. Parameters are the same as in Fig. 4. The dot-dashed and dashed lines are model calculations for volume and surface scattering without corrections, respectively. The thin solid line corresponds to surface scattering model with the corrections of extinction in the cavity or variable optical depth for scattering (see text). The employed parameters are summarized in Table 3. These lines are normalized to the observed data at the distance of $22'$

polarization, up to 64%, is observed in the northernmost and southernmost region, coincident with the edges of the diffuse component. The large degree of polarization and the centrosymmetric pattern of polarization vectors indicate that the polarization mechanism is scattering and that the diffuse component is illuminated by a source located at the polarization center. Although the polarization vectors (Fig. 1) do not form a complete centrosymmetric pattern, most of the normals of the po-

Table 3. Parameters of the model calculations

	R_0 or Z_0^a (arcsec)	$i(^{\circ})^b$	$C(\text{arcsec}^{-1})^c$	Expressed lines	
				Figure 4	Figure 5
Volume scattering	–	35	0.20	Dot-dashed	Dot-dashed
Surface scattering	–	35	0.20	Dashed	Dashed
Surface scattering with variable optical depth	33	16	0.28	Dashed	Thin solid
Surface scattering with finite extinction	80	30	0.25	Dashed	Thin solid

^a R_0 for finite extinction and Z_0 for variable optical depth

^b Inclination angle of the nebula from the plane of the sky

^c Coefficient of the paraboloid; $Z = C(X^2 + Y^2)$

larization vectors converge at a position immediately close to IRS 2, which coincides with an ultra-compact H II region (Rodríguez et al., 1980) and IRAS source 18162-2048. (see Sect. 3.3).

The northern lobe is brighter than the southern one, which would be obscured by the tilted disk discussed in Sect. 3.2. The inclination is consistent with that expected from the CO bipolar flow (Yamashita et al., 1987); the disk would be tilted in the way that nearer side is in the south because the blue- and red-shifted lobes of the flow are in the north and south, respectively.

The degrees of polarization in the L' band (Fig. 2) are comparable to or slightly larger than those in the K band (Fig. 1), in contrast to the wavelength dependence for interstellar polarization (Serkowski et al., 1975) or for most cases of infrared polarization of YSOs measured on the position of the peak intensity (Dyck and Capps, 1978; Heckert and Zeilik, 1981). Generally, for scattered radiation polarization at longer wavelengths shows larger degrees than at shorter wavelengths due to the following two reasons. (i) The integrated polarization is reduced by multiple scattering at shorter wavelength. (ii) Polarization in the L' band produced by single scattering is comparable to or slightly larger than that in the K band, in the wavelength range of $\lambda > 2\pi a$ (van de Hulst, 1957; Matsumura and Seki, 1986). In previous measurements of YSOs on the intensity peak, contamination from thermal emission has resulted in a wavelength dependence showing smaller polarization at longer wavelengths (Dyck and Capps, 1978; Heckert and Zeilik, 1981).

In the extended region of Cep A, the polarization in the L band is much higher than that in the K band (Joyce and Simon, 1986); they attributed the relation to multiple scattering. In the diffuse component of GGD27 IRS, we argue that single scattering must be the dominant process because of the near equality of polarization in the K and L' bands.

The radial dependences of both the degree of polarization and surface brightness in the K band along the vertical line to the north from IRS 2 are shown in Figs. 4 and 5. The effect of beam size on the degree of polarization, which is due to the variation of position angles within the beam, was calculated for a centrosymmetric field of polarization vectors for the cases of both a constant and a r^{-2} -dependent surface brightness, and was shown to be negligibly small 20'' away from IRS 2. Both the polarization and the surface brightness inside 20'' appear to be heavily affected by the presence of a disk and this will be dis-

cussed later in this section. Figure 4 shows that the degree of polarization increases with distance from IRS 2.

We made a model-fitting for this infrared reflection nebula by adopting a paraboloidal shape, $Z = C(X^2 + Y^2)$, where X and Y axes are in the plane of the disk, tilted with an angle, i , from the plane of the sky, with C and i free parameters. We assume (i) single and (ii) Rayleigh scattering ($x = 2\pi a/\lambda \ll 1$) and neglect thermal emission. According to the calculation with Mie scattering (Matsumura and Seki, 1986) Rayleigh scattering approximation holds for $a < 0.35 \mu\text{m}$ at $\lambda = 2.2 \mu\text{m}$ for each of graphite, silicate, and ice grains. The assumption of single scattering is supported by the near equality of K and L' band polarization degrees at a level larger than 20%. First, we make an assumption that the extinction is negligibly small and the scattering cross section is constant per unit volume or per unit area. We calculated two cases of the spatial distribution of the scattering material. We call them (i) volume scattering and (ii) surface scattering (Nagata et al., 1986); that is, (i) scattering occurs on grains inside the lobes and (ii) scattering occurs only at the surface of the shell enclosing the cavity. The latter model is based on the shell structure recently reported for a CO bipolar flow in the L1551 dark cloud (Snell et al., 1985; Uchida et al., 1987).

Systematic search of parameters C and i shows a general tendency: the surface scattering model (dashed line in Fig. 4) gives a good agreement with the observed radial dependence of polarization, whereas the volume scattering model (dot-dashed line) does not rise sufficiently steeply. This can be simply understood as follows: the degree of polarization due to volume scattering is an average of polarization by dust grains located along the line of sight, and so the polarization changes little with the projected radial distance. That due to surface scattering is an average of the polarization at the two points of the paraboloid which the line of sight intersects. Therefore, the curve of surface scattering model shows a gradient steeper than that of the volume scattering.

It should be noted that we can determine the parameters C and i uniquely, because the vertical shift and the gradient of the curve are sensitive to i and C , almost independently. Consequently, we obtained parameters, $i = 35^{\circ}$ and $C = 0.20 \text{ arcsec}^{-1}$, for the best fit to the observed radial dependence of polarization.

In spite of this agreement of the surface scattering model with the polarization result, it shows a substantial deviation from the observed brightness distribution (Fig. 5). Then we introduce

either (i) height(Z)-dependence of optical depth for scattering, for instance, due to grain density variation, as $\exp(-Z/Z_0)$, or (ii) extinction of light during the transmission through the cavity as $\exp(-R/R_0)$. Case (i) with parameters, $i = 16^\circ$, $C = 0.28 \text{ arcsec}^{-1}$, and $Z_0 = 33''$, and case (ii) with parameters, $i = 30^\circ$, $C = 0.25 \text{ arcsec}^{-1}$, and $R_0 = 80''$ provide radial dependence of surface brightness in good agreement with observation (thin solid line in Fig. 5) and that of polarization similar to that derived previously. If case (ii) applies, the characteristic mean-free-path, $R_0 = 80''$, corresponds to a density of about 10^4 cm^{-3} , which may be too high for the cavity. However, the actual dust shell must have transient region inside and the extinction would occur therein. The resultant shape of the cavity with the parameters $C = 0.28$ or 0.25 arcsec^{-1} fits fairly well to the K band surface brightness (dashed line in Fig. 1 is for $C = 0.28$), and the small inclination angle ($i = 16^\circ$ or 30°) is also consistent with the fact that the source appears to be viewed from nearly edge-on.

Thus a simple model that a single Rayleigh scattering occurs on the inner surface of a paraboloidal shell can provide good agreement with the observed radial dependences of both polarization and surface brightness. This geometry of scattering is in good agreement with the shell structure of the bipolar flow, suggesting that the infrared light is scattered by the dust shell formed by the molecular outflow. The good agreement of the spatial extent between the infrared reflection nebula and the CO bipolar flow (Yamashita et al., 1987) also supports this idea.

Within $20''$ from IRS 2, which we have neglected in the previous discussions, the degrees of polarization are larger than those calculated for the surface scattering model (Fig. 4). This could be attributed to a contribution from volume scattering, arising from a higher density of dust grains around the central star.

Deviations from a centrosymmetric pattern are seen in three regions in Fig. 1. First is a region around IRS 4, where the degree of polarization is small. This is probably due to dilution by the infrared light from IRS 4, which corresponds to both an optical nebulosity GGD 27 itself and No. 41 on the CCD image by Hartigan and Lada (1985). Therefore, IRS 4 (GGD 27) would not be a bright knot in the infrared reflection nebula but a self-luminous source. Second is a region to the northeastern side of IRS 2, where surface brightness decreases steeply to the east. The polarization integrated over the beam would be dominated by the contribution from the western part of the beam and, as a result, the normals of the polarization vector point to IRS 2 from the western part of the beam, not from the center. Third is a region to the west of IRS 1, where the polarization vectors are almost vertical (P.A. $\sim 0^\circ$), different from those expected for an illumination by IRS 2. Their normals pointing to IRS 1, together with the enhancement of brightness here, means that a reflection nebulosity is likely to be also associated with IRS 1.

3.2. The disk

It is striking that not just the surface brightness, but also the degree of polarization, decreases both east and west of IRS 2. The degree of polarization can be reduced by 1) an addition of thermal emission by hot dust or free electrons, 2) contamination by background stars, or 3) multiple scattering by dust grains. The reduction in surface brightness as well as polarization would exclude cases 1) and 2). Multiple scattering by dust grains is therefore the most plausible and suggests the presence of a dense

condensation extended in the east-west direction, that is, perpendicular to the elongation of the surface brightness. Comparison of the surface brightness distribution in the K and L' bands also supports this interpretation: since the extinction coefficient decreases with increasing wavelength, as was discussed in Sect. 3.1., the dips in either side of IRS 2 in the L' band are shallower than those in the K band.

The extent of the disk can be obtained from the distribution of polarization and surface brightness. If we assume that polarization is caused by scattering and that depolarization is due to multiple scattering, then a small degree of polarization delineates the high density region. The region within $30''$ to the west of IRS 2 shows polarization less than 5%, while the polarization at a point $45''$ away is as large as 15% in the K band (Fig. 1). Thus the radius of the disk is estimated to be about $30''$ or 0.25 pc in the east-west direction. From the decrease of surface brightness toward the central source from the north, the height of the disk is inferred to be about $20''$. We obtain therefore a rough size (diameter \times thickness) of $60'' \times 40''$ for the obscuring material.

We estimate the extinction in the disk using the same method as that employed by Lenzen et al. (1984), that is, by comparing the photometric data with the intrinsic (unobscured) magnitude of the central source. They took account of the effects of the albedo of the dust grains and of the solid angle of conical lobe, in converting the total integrated flux over the nebula into an intrinsic flux of the central star. We use the brighter northern lobe only in the calculation of the intrinsic flux, both because the southern lobe contains an additional source, IRS 1, and because it may suffer from an additional extinction by the slightly tilted disk. If we assume an albedo of 22% in the K band (Mathis et al., 1983) and a solid angle of 3.6 sterad (corresponds to an aperture angle of 130°) for the northern lobe, the intrinsic flux originating from the central illuminating source is estimated to be $2.1 \cdot 10^{-15} \text{ W cm}^{-2} \mu\text{m}^{-1}$. Comparing this value with the photometry of IRS 2, we obtain an extinction of 6.2 mag in the K band or a visual extinction of 75 mag, if we assume the extinction curve No. 15 of van de Hulst (Johnson, 1968). Adopting the relationship, $N(\text{H}_2) = 1.3 \cdot 10^{21} \times A_V$ (Dickman, 1978), this amount of extinction yields a column density $N(\text{H}_2) \sim 1.0 \cdot 10^{23} \text{ cm}^{-2}$, which, using the size of the disk obtained above, leads to a density of $1.3 \cdot 10^5 \text{ cm}^{-3}$ and a mass of the disk of $200 M_\odot$.

Recent CS emission maps revealed a dense ($8 \cdot 10^4 \text{ cm}^{-3}$) cloud elongated ($70'' \times 30''$) in the direction of east-west (Yamashita et al., 1986). The values are in good agreement with those estimated from the infrared observation.

3.3. GGD 27 IRS 2

We have shown that, from the centrosymmetric pattern of the polarization vectors, the illuminating source of the reflection nebula is IRS 2. The radio continuum source revealed with the VLA (Rodríguez et al., 1980) is coincident with IRS 2 within a positional error of $2''$. The IRAS source, 18162-2048, which is identified with GL 2121 in the IRAS point source catalogue, also coincides with that of IRS 2. The position of the far-infrared source, GL 2121, is considerably different from that of IRS 2 by 0.9 arcmin in R.A. and 3.9 arcmin in Dec. (Walker and Price, 1975). However, GL 2121 probably corresponds to IRS 2 if we take the positional uncertainty of the AFGL rocket survey into consideration.

The spectral energy distribution of IRS 2, including the IRAS data, is shown in Fig. 3. It can be decomposed, after a correction of $A_V = 20$ mag, into three components, of > 6000 K, 800 K, and around 70 K; the three components each dominate a different wavelength range. The corrected spectrum in the near-infrared can be fitted with any temperature above 6000 K, being consistent with the spectral type of B1V derived for an exciting source by Rodriguez et al. (1980). The 800 K component would arise from thermal emission from hot dust located close to the exciting source rather than from free-free emission because the infrared flux is much larger than that expected from the radio flux at 5 GHz. The far-infrared component (~ 70 K) shows a rather broad spectral distribution ranging from 40 K through 110 K of color temperature, depending on which of the wavelengths 12, 25, 60, and $100 \mu\text{m}$ are used in computation; we assume dust emissivity proportional to λ^{-1} .

The integrated flux from 1 to $100 \mu\text{m}$ corresponds to a luminosity of $20000 L_\odot$ at the assumed distance of 1.7 kpc, much larger than the $6000 L_\odot$ assigned to a B1V star by Rodriguez et al. (1981). The same authors noted the possibility that the spectral type B1V is a lower limit because of (i) the direct absorption of UV photons by grains or of (ii) a lower temperature for a more luminous star in a pre-main-sequence stage. If we take the luminosity of $20000 L_\odot$ for IRS 2, it corresponds to a spectral type of B0V or B0.5V.

The visual extinction of 20 mag obtained from the photometry apparently does not agree with the extinction of 75 mag obtained in Sect. 3.2. It should be noted, however, that the former determination of extinction ($A_V \sim 20$ mag) involves the tacit assumption that all the photons coming toward us are transmitted through the disk from the central star not scattered. However, the large polarization ($P = 21.1 \pm 0.1\%$) toward the central source, comparable to that of the diffuse component near IRS 2 (Fig. 4), means that a substantial fraction of the flux actually arises from scattering above the disk. As a result, the apparent spectrum would be substantially modified by the scattered light: the color suffers "blueing" in the near-infrared regions because of (i) less extinction through a low-density cavity and (ii) higher scattering efficiency at shorter wavelengths.

Similar apparent disagreement between the extinctions derived by the different ways or at different wavelengths was reported. Persson and Frogel (1974) derived extinctions of K3-50 by comparing fluxes of ratio continuum, hydrogen lines, and H band continuum with the decrease of the extinctions at shorter wavelengths. Harvey et al. (1977) measured FIR fluxes of NGC 6334 and the Rosette nebula and derived the optical thickness of $0.1 \sim 0.5$ or $A_V > 20 \sim 100$ mag, which is inconsistent with the visible nebulosities. Both authors suggested the models similar to us, that is, spatially varying obscuration (Persson and Frogel, 1974) or cylindrically symmetric distribution of the dust with a hole pointing to the nebulosities (Harvey et al., 1977). Thus, such anisotropic phenomena may be universal among young sources. Therefore, it would not be an appropriate way to obtain extinctions toward the central stars in star forming regions from near-infrared photometry, especially for highly polarized sources.

3.4. GGD 27 IRS 1

The results of the photometry of IRS 1 are summarized in Table 2 and displayed in Fig. 3. The spectrum is consistent with

a star (> 4000 K) suffering visual extinction of 30 mag and showing little indication of hot dust emission. This large visual extinction indicates that IRS 1 would be located within or beyond the cloud to which IRS 2 belongs. IRS 1 is supposed to be associated with its own nebulosity not the one around IRS 2, because the polarization vectors show little deviations from the centrosymmetric pattern centered on IRS 2, as was discussed in Sect. 3.1. The CCD image by Hartigan and Lada (1985) has a star-like image (No. 32; see Table 1) at the position coincident with IRS 1 within the positional error. Its brightness in the R and I bands is 21.3 and 19.6 mag, respectively. Thus its color, $R-I = 1.8$ mag, is much bluer than the color, $J-K = 5.0$ mag of IRS 1. The positional coincidence would be by chance and IRS 1 is unlikely to be No. 32.

4. Conclusions

The main results derived from K and L' polarization maps of the infrared reflection nebula GGD 27 IRS are summarized as follows.

1. From the centrosymmetric pattern of the polarization vectors the illuminating source is shown to be IRS 2.
2. A surface scattering model can explain the radial dependences of both the degree of polarization and surface brightness.
3. Weak surface brightness and small polarization to both east and west of IRS 2 (compared with those to north and south) indicate the presence of a disk elongated in the east-west direction.
4. The size and the mass of the disk are estimated to be $60''$ (E-W) \times $40''$ (N-S) or $(0.5 \text{ pc} \times 0.3 \text{ pc})$ and $200 M_\odot$, respectively.
5. The near-infrared flux of IRS 2 within an $8''$ beam is substantially dominated by scattered radiation, rather than by radiation transmitted through the disk from the central source.

Acknowledgements. We thank the staff of the United Kingdom Infrared Telescope and Institute for Astronomy, University of Hawaii for their support and hospitality. We are grateful to Drs. M. Tanaka and N. Ukita for careful reading of this manuscript. We also acknowledge Prof. H. Hasegawa and Dr. N. Kaifu for their continuous encouragement. This work was supported by the SERC and the Ministry of Education, Science, and Culture of Japan.

References

- Castelaz, M.W., Hackwell, J.A., Grasdalen, G.L., Gehrz, R.D., Gullixson, C.: 1985, *Astrophys. J.* **290**, 261
 Dickman, R.L.: 1978, *Astrophys. J. Suppl.* **37**, 407
 Dyck, H.M., Capps, R.W.: 1978, *Astrophys. J. Letters* **220**, L49
 Gyulbudaghian, A.L., Glushkov, Yu.I., Denisjuk, E.K.: 1978, *Astrophys. J. Letters* **224**, L137
 Hartigan, P., Lada, C.J.: 1985, *Astrophys. J. Suppl.* **59**, 383
 Harvey, P.M., Campbell, M.F., Hoffmann, W.F.: 1977, *Astrophys. J.* **215**, 151
 Heckert, P.A., Zeilik II, M.: 1981, *Astron. J.* **86**, 1076
 Heckert, P.A., Zeilik II, M.: 1984, *Astron. J.* **89**, 1379
 Heckert, P.A., Zeilik II, M.: 1985, *Astron. J.* **90**, 2291
 Hodapp, K.-W.: 1984, *Astron. Astrophys.* **141**, 255
 Joyce, R.R., Simon, T.: 1986, *Astron. J.* **91**, 113

- Johnson, H.L.: 1968, in *Nebulae and Interstellar Matter*, eds. B.M. Middlehurst, L.H. Aller, p. 167, *Univ. Chicago Press*, Chicago
- Lenzen, R., Hodapp, K.-W., Solf, J.: 1984, *Astron. Astrophys.* **137**, 202
- Lonsdale, C.J., Dyck, H.M., Capps, R.W., Wolstencroft, R.D.: 1980, *Astrophys. J. Letters* **238**, L31
- Mathis, J.S., Mezger, P.G., Panagia, N.: 1983, *Astron. Astrophys.* **128**, 212
- Matsumura, M., Seki, M.: 1986, *Astrophys. Space Sci.* **126**, 155
- Nagata, T., Yamashita, T., Sato, S., Suzuki, H., Hough, J.H., Garden, R., Gatley, I.: 1986, *Monthly Notices Roy. Astron. Soc.* 223,7P
- Persson, S.E., Frogel, J.A.: 1974, *Astrophys. J.*, **188**, 523
- Rodriguez, L.F., Moran, J.M., Ho, P.T.P., Gottlieb, E.W.: 1980, *Astrophys. J.* **235**, 845
- Rodriguez, L.F., Carral, P., Ho, P.T.P., Moran, J.M.: 1982, *Astrophys. J.* **260**, 635
- Sato, S., Nagata, T., Nakajima, T., Nishida, M., Tanaka, M., Yamashita, T.: 1985, *Astrophys. J.* **291**, 708
- Sato, S., Tamura, M., Nagata, T., Kaifu, N., Hough, J., McLean, I.S., Gatley, I.: 1987, *Monthly Notices Roy. Astron. Soc.* (in press)
- Serkowski, K., Mathewson, D.S., Ford, V.L.: 1975, *Astrophys. J.* **196**, 261
- Snell, R.L., Bally, J., Strom, S.E., Strom, K.M.: 1985, *Astrophys. J.* **290**, 587
- Tokunaga, A.T., Lebofsky, M.J., Rieke, G.H.: 1981, *Astron. Astrophys.* **99**, 108
- Uchida et al.: 1987, (in preparation)
- Van de Hulst, H.C.: 1957, *Light Scattering By Small Particles*, John Wiley and Sons, Inc., New York
- Walker, R.G., Price, S.D.: 1975, *AFGL Infrared Sky Survey* AFGL-TR-75-0373
- Werner, M.W., Dinerstein, H.L., Capps, R.W.: 1983, *Astrophys. J. Letters* **265**, L13
- Yamashita, T., Tamura, M., Sato, S., Suzuki, H., Kaifu, N., Mountain, C.M., Moore, T.: 1987, (in preparation)